Geophysical Research Letters

RESEARCH LETTER
10.1029/2018GL079576

Key Points:
- All the red sprites observed over Hurricane Matthew on two nights were produced by positive cloud-to-ground lightning strokes
- All the sprite-parent CG strokes were located in the outer rainbands as defined by the relatively cold cloud top brightness temperature; none were in the inner core
- The observations are contrary to ISUAL observations showing the dominance of negative sprite-producing CG strokes in the region of interest

Correspondence to:
G. Lu,
gaopenglu@gmail.com

Citation:
Huang, A., Lu, G., Yue, J., Lyons, W., Lucena, F., Lyu, F., et al. (2018). Observations of red sprites above Hurricane Matthew. *Geophysical Research Letters*, *45*. https://doi.org/10.1029/2018GL079576

Received 11 JUL 2018
Accepted 3 NOV 2018
Accepted article online 9 NOV 2018

Observations of Red Sprites Above Hurricane Matthew

Anjing Huang[1,2], Gaopeng Lu[1,3,4], Jia Yue[5], Walter Lyons[6], Frankie Lucena[7], Fanchao Lyu[8], Steven A. Cummer[8], Wenjuan Zhang[9], Liangtao Xu[9], Xianghui Xue[10], and Shuang Xu[10]

[1]Key Laboratory of Middle Atmosphere and Global Environment Observation, Institute of Atmospheric Physics,Chinese Academy of Sciences, Beijing, China, [2]College of Earth and Planetary Sciences, University of Chinese Academy of Sciences, Beijing, China, [3]State Key Laboratory of Numerical Modeling for Atmospheric Sciences and Geophysical Fluid Dynamics, Institute of Atmospheric Physics, Chinese Academy of Sciences, Beijing, China, [4]Collaborative Innovation Center on Forecast and Evaluation of Meteorological Disasters, Nanjing University of Information Science and Technology, Nanjing, China, [5]Department of Atmospheric and Planetary Sciences, Hampton University, Hampton, VA, USA, [6]FMA Research, Ft. Collins, CO, USA, [7]Cabo Rojo, Puerto Rico, [8]Electrical and Computer Engineering Department, Duke University, Durham, NC, USA, [9]State Key Laboratory of Severe Weather, Chinese Academy of Meteorological Sciences, Beijing, China, [10]School of Earth and Space Sciences, University of Science and Technology of China, Hefei, China

Abstract More than three dozen red sprites were captured above Hurricane Matthew on the nights of 1 and 2 October 2016 as it passed to the north of Venezuela after undergoing rapid intensification. Analyses using broadband magnetic fields indicate that all of the sprites were produced by positive cloud-to-ground (CG) strokes located within the outer rainbands as defined by relatively cold cloud top brightness temperatures (≤194 K). Negative CG strokes with impulse charge transfers exceeding the threshold of sprite production also existed, but the timescale of the charge transfer was not sufficiently long to develop streamers. The reported observations are contrary to the finding of the Imager of Sprites/Upper Atmospheric Lightning showing that sprites are preferentially produced by negative strokes in the same geographic region. Further ground-based observations are desired to obtain additional insights into the convective regimes associated with the dominance of negative sprites in many oceanic and coastal thunderstorms.

Plain Language Summary The contribution from citizen scientists has been greatly helpful for extending the scope of basic scientific research to the broad community. Thanks for the night sky photographer living in Puerto Rico, Frankie Lucena, more than three dozen red sprites were captured on both the long-exposure DSLR camera and the low-light-level video camera, forming a very valuable data set to examine the sprite genesis above tropical cyclones. The comparison with coordinated broadband sferic measurements made at more than 2,000-km range near Duke University indicates that all of these sprites were produced by positive cloud-to-ground strokes located in the outer rainband region. None of these sprites were produced above the inner core region of the hurricane. The fact that all the sprites observed above Hurricane Matthew are positive events is contrary to the spaceborne observations of the Imager of Sprites/Upper Atmospheric Lightning (ISUAL) over the past 12 years (2004–2015) that almost all the sprites observed by ISUAL in the similar geographic region were of negative polarity. Therefore, it is worthwhile conducting the ground-based observation of sprites in this region to document the thunderstorms responsible for the population of negative sprites over oceanic thunderstorms.

1. Introduction

There is increasing interest to understand the impact of thunderstorms and associated lightning activity on the lower ionosphere (Davis & Johnson, 2005; Shao et al., 2013; Yu et al., 2017). Major impacts include lightning-induced transient luminous events in the mesosphere, such as red sprites (Sentman et al., 1995), gigantic jets (Liu, Spiva, et al., 2015; Pasko et al., 1997), and elves (Taranenko et al., 1993). During the past two decades, the observational studies on sprites mainly focused on continental thunderstorms (e.g., Boccippio et al., 1995). Mesoscale convective systems (MCSs) have been recognized as the main sprite producer in North America (Lyons, 1996), Europe (Neubert et al., 2005; Soula et al., 2009), and mainland of China (Huang et al., 2018; Su et al., 2002). Previous observations consistently indicate that positive cloud-to-ground (+CG) strokes, typically produced within the trailing stratiform (e.g., Lu et al., 2013), are by far the predominant producer of sprites above MCSs.

Although the vast majority (>90%) of lightning occurs over land (Christian et al., 2003), oceanic CG strokes generally have higher peak currents and larger charge moment changes than those over land (Füllekrug et al., 2002; Said et al., 2013). Therefore, the CG strokes produced by oceanic/coastal thunderstorms could be more efficient in driving electromagnetic coupling between troposphere and middle atmosphere. Indeed, the spaceborne observations of the Imager of Sprites/Upper Atmospheric Lightning (ISUAL) show that the difference between land and ocean in the sprite production is not as distinct as that for lightning (Chen et al., 2008), which is also shown by the surveys by measuring the transient Schumann resonance (Füllekrug et al., 2002; Sato & Fukunishi, 2003). In particular, a considerable fraction (~18%) of ISUAL-observed sprites is produced by negative CG strokes spawned in oceanic/coastal thunderstorms (Lu et al., 2017). Therefore, the scarcity of negative sprites in the ground-based observations over continents is likely a consequence of the differences between continental and oceanic thunderstorms in spawning negative strokes with characteristic charge transfer capable of producing sprites.

Tropical cyclones (TCs), as large-scale convective systems originating over oceans, often bring heavy precipitation. Although TCs typically produce less lightning than most deep tropical convections, they on occasion can generate plentiful lightning within both the outer rainbands and inner core (Lyons & Keen, 1994). As shown by Wu et al. (2017), the relationship between TC lightning and storm intensification does hold promise for its predictive value but is extremely complex. Even less is known about the circumstance in which TC lightning possesses characteristics suitable for sprite production. Huang et al. (2012) mentioned the observation of numerous sprites above Typhoon Lionrock in 2010, but unfortunately, their analyses focused on gigantic jets. Thomas et al. (2010) investigated the lightning activity in three North Atlantic hurricanes in 2005 to evaluate the capability of TCs to produce elves and sprites, indicating that the inner core area does not spawn considerable sprite-producing CGs. However, previous studies showed that most lightning in hurricanes is found in the vicinity of outer spiral rainbands (Molinari et al., 1999), although the lightning activity in the inner core area is potentially a better indicator for predicting the rapid intensification of TCs (e.g., Zhang et al., 2015). So could the outer rainbands of TCs be the main region of sprite production?

In this paper, we examined the observations of sprites over Hurricane Matthew as the deadliest, and also the southernmost category-5 Atlantic hurricane since 2005 by causing over 600 deaths while making landfalls across the central Caribbean and southeastern seaboard of United States (Miller et al., 2018). Matthew rapidly intensified from categories 1 to 5 on 30 September 2016. On the nights of 1 and 2 October, night sky photographer Frankie Lucena captured about 40 sprites over Matthew, providing an unanticipated opportunity to gain more insights into the phenomenology of sprite production from hurricane convection in tropical oceans.

2. Observations and Analysis

Hurricane Matthew reached a peak intensity of 145 knots at 00UTC (Coordinated Universal Time) on 1 October (Stewart, 2017). Both the beginning and ending of a 24-hr rapid intensification period were accompanied by bursts of lightning in the eyewall as detected by the World-Wide Lightning Location Network (WWLLN; Abarca et al., 2010). Drifting with the weak steering currents, Matthew slowly weakened to a category-4 hurricane, with estimated intensity ranging between 125 and 135 knots by 18UTC on 2 October, when the 850- to 200-mb vertical wind shear remained at a moderate level (15–20 knots). Along with a declining trend, heavy rain and vigorous convection in the east portion of the hurricane were associated with plentiful lightning (Stewart, 2017). During the weakening phase when the vertical wind shear at upper levels was intensified to cause an asymmetric evolution, totally 42 red sprites were observed, including 31 sprites between 0436UTC and 0840UTC on 1 and 11 October events from 0201UTC to 0343UTC on 2 October. The ratio (36 of 42, or ~86%) of sprites with causative CGs detected by WWLLN is similar to the sprite observations in the continental United States and North China, where the sprite-producing CGs are located by WWLLN with accuracy typically better than 10 km (Huang et al., 2018). As shown in Figure 1b, these sprite-producing strokes occurred to the north of Venezuela, at range of 500–800 km from the observation site. Figure 1a shows the long-exposure (over 1 s at ISO-6400) color picture (photographed with a Canon REBEL T3 DSLR) of a bright sprite observed at 0656UTC on 1 October, with the causative stroke being 593 km from the observer. In the background we can see stars and also the mesopause gravity wave (banded structure) related to the convection of hurricane (Miller et al., 2018). The maximum range of sprite observation is estimated to be >800 km.

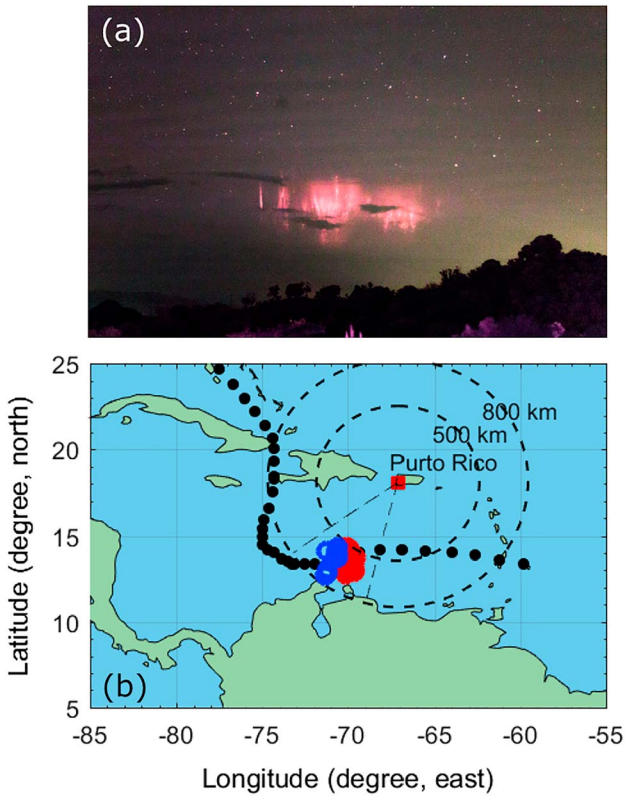

Figure 1. (a) Red sprite cluster over Hurricane Matthew recorded by Frankie Lucena from Cabo Rojo, Puerto Rico, on the night of 1 October 2016. (b) Location of parent lightning strokes detected by World-Wide Lightning Location Network for the sprites observed over Matthew (red and blue circles mark the strokes on 1 and 2 October, respectively). The elevation of the observation site (18.05°N, 67.11°W) is about 67 m (above mean sea level), and the black dots mark the track of Matthew since its early organization near Barbados on 28 September and until it reached the Bahamas on 7 October.

All the sprite-producing strokes are located at ranges between 2,550 and 2750 km from Duke Forest, where the broadband magnetic fields were recorded with two pairs of induction coils whose frequency range is $<$0.1 to 400 Hz (referred to as ultralow frequency, ULF) and 50 to 25 kHz (very low frequency, VLF), respectively (e.g., Lu et al., 2013). Our analysis mainly refers to the ULF signals to estimate the impulse charge moment change (iCMC, defined as the product of charge transfer to ground within 2 ms after the return stroke and the original height in thunderclouds) as an effective metric to evaluate the capability of a CG stroke to produce sprite (Lu et al., 2012). Cummer and Lyons (2005) examined three thunderstorms in central United States and found that the threshold of positive sprite-producing iCMCs vary between +350 and +600 C-km from night to night probably due to the variability in the nighttime mesospheric condition (Qin et al., 2013).

Figure 2 shows the distribution of WWLLN lightning (within 1-hr interval centered at the time given in each panel) overlaid on the cloud field of Matthew at four different times, using the inferred cloud top temperatures from the infrared brightness data (equivalent blackbody temperature with spatial resolution of 4 km $\times$ 4 km) merged from all available geostationary satellites (e.g., GOES-8/10, METEOSAT-7/5, and GMS). The sprite-producing strokes are indicated with red *plus* signs. We can see that the lightning activity is present in both the eyewall and outer rainbands, and the lightning discharges detected by WWLLN in outer rainbands outnumber that in the eyewall (e.g., Lyons & Keen, 1994; Zhang et al., 2015). However, sprites were only observed above the outer rainbands with higher lightning occurrence. As shown in Figure 2, the sprite-producing CGs are generally located in the coldest cloud region where the infrared brightness temperature ranges between 183 and 194 K.

We also consider the possibility that any sprites produced over the eyewall had been missed in the observations. On the night of 1 October, the most distant sprite-producing stroke was about 670 km from the observer, while the eyewall was within 800-km range. As shown in Figure 1b, the sprites recorded on 2 October were above a farther region from the observer (with the farthest distance of about 749 km), and these sprites still appear relatively high in the field of view. Therefore, we can comfortably exclude the chance that any visible sprites have been produced by lightning in the inner core region.

The analyses of 11 sprites observed on the night of 2 October, when Matthew remained category 4 while the lightning activity in the hurricane has been significantly reduced, give the same results on the location of sprite-producing strokes with respect to the spatial structure of hurricane. All the sprite-producing strokes detected by WWLLN are located in the outer rainbands as defined by the relatively cold cloud top brightness temperature $\leq$194 K.

Previous observations reveal that sprite-producing CG strokes are predominately produced in the trailing stratiform of MCSs (Boccippio et al., 1995; Lu et al., 2013; Lyons, 1996), which are usually confined by cloud top brightness temperature of 220–225 K (or radar reflectivity of 15–35 dBZ; Huang et al., 2018; Soula et al., 2009; Yang et al., 2013). According to satellite images of brightness temperature shown in Figure 2, the outer rainbands spawning sprite-producing CGs have the quasi-circular structure similar to MCSs (e.g., Harr & Elsberry, 1996). By examining the image sequence of brightness temperature, we can see that the overall structure of Matthew did not evolve very much from 1 October to 4 October when the intensity (or the maximum wind speed) of Matthew remained relatively steady. Therefore, we refer to the ARSR-4 radar reflectivity data (dBZ) from Guantanamo Bay, Cuba, on 4 October (Stewart, 2017), which shows a spiral convective line corresponding to the lightning activity in the eye-wall region. Due to the significantly more lightning discharges detected by WWLLN, the outer rainbands of Matthew with dominance in spawning sprite-producing strokes might be characterized by relatively high reflectivity (e.g., $>$40 dBZ; Didlake & Kumjian, 2017),

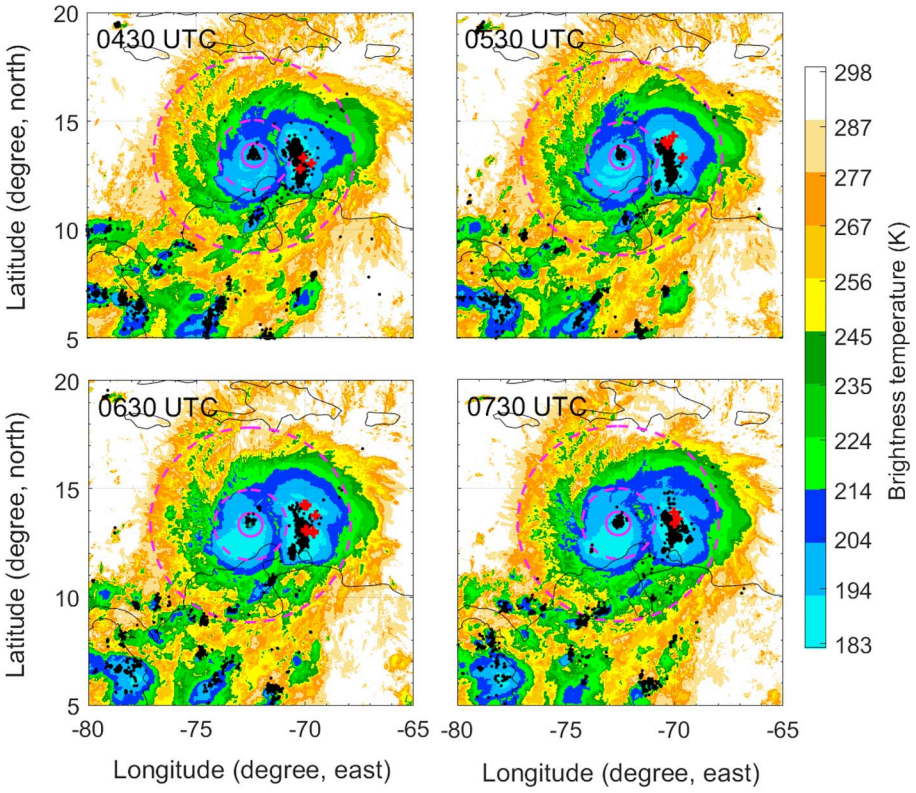

Figure 2. Distribution of World-Wide Lightning Location Network lightning (black dots) in Matthew as shown by the combined satellite observation of infrared brightness temperature during four consecutive time intervals centered at the image time. All the sprite-producing strokes (red pluses) detected by World-Wide Lightning Location Network are located in the outer rainband region with infrared brightness temperature below 194 K. The pink dashed circles mark the circular region with radius of 50, 200, and 500 km centered at the eye core.

implying the local presence of considerable convection (Houze, 2010; Xu et al., 2014), which might explain the relatively low cloud top brightness temperature for the sprite-producing region of Matthew in comparison with the trailing stratiform of MCSs. In comparison, all the gigantic jets examined by Huang et al. (2012) were produced in the eyewall convective region of Typhoon Lionrock; Liu, Spiva, et al. (2015) reported the observation of seven upward electrical discharges (including four gigantic jets) above the convective region of Tropical Depression Dorian.

3. Estimate of Sprite-Producing Lightning Strength

We select the sprite event shown in Figure 1a as an example to estimate the strength of sprite-producing CG strokes, which can be quantitatively evaluated by using both peak current and iCMC. According to the image fields captured with a Watec 902H Ultimate video camera at 30 frames per second, this sprite was a dancing event consisting of two elements (shown with different colors in the inset of Figure 3a) that were produced by two strokes both detected by WWLLN. The parent CG stroke of the first element was the strongest CG observed on 1 October. The estimated iCMC for this sprite-producing stroke is about +825 C-km; the peak current estimated from the VLF data (Figure 3c) using the method given by Lu et al. (2017) is about +148 kA. As shown in Figure 3b, both sprite elements were sufficiently bright to induce the so-called *sprite current* signature that is characterized as a slow magnetic pulse of millisecond scale without an associated fast VLF impulse (Cummer et al., 1998; Pasko et al., 1998). The observation of a sprite current signal indicates that the timescale of sprite-producing charge transfer should be at least 2 ms. Note that despite a weaker parent stroke (with peak current of +79 kA and iCMC of +350 C-km), the sprite current signal for the second element (which also appears to be brighter) is stronger than the first sprite element (by a factor of about 2.5) and even the corresponding causative stroke. This implies that either

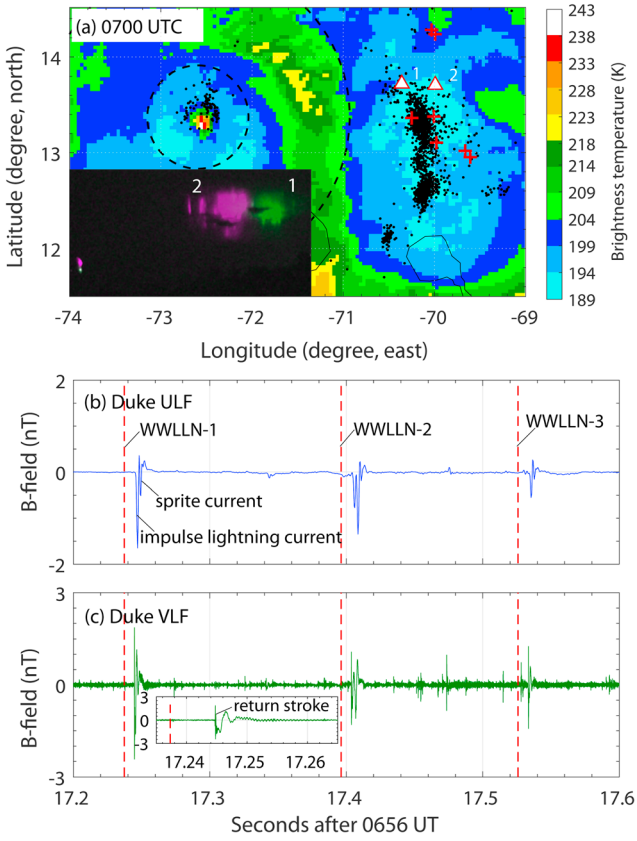

Figure 3. Analysis of a dancing sprite with two elements (shown with different colors in the inset image of panel a) observed at 0656:17UTC over Matthew. (a) The black dots and red *plus* symbols overlaid on the base map of brightness temperature respectively represent World-Wide Lightning Location Network (WWLLN) lightning and sprite-producing strokes within 1-hr interval centered at 0700UTC. The two sprite elements were produced by different strokes (marked with triangles) that are separated by about 60 km. (b) Both sprite elements induced the *sprite current* signal shown in the ultra-low-frequency (ULF) magnetic field recorded at 2,634-km range. (c) the very-low-frequency (VLF) signal recorded near Duke University for the parent stroke of the first sprite element is plotted, showing the fast impulse from the return stroke.

the preceding sprite occurrence and/or a possible long continuing current after the first sprite-producing stroke might make the mesospheric environment more favorable for sprite production. In addition, the gravity waves discernible in the long-exposure DSLR image may cause inhomogeneities in the upper mesosphere favorable for sprite initiation (Liu, Dwyer, et al., 2015; Liu et al., 2016; Marshall et al., 2015; Qin et al., 2012; Yue & Lyons, 2015).

The WWLLN also detected a third stroke (with estimated peak current of +87 kA) of that was not associated with an optical sprite observation, and thus, its iCMC (about +250 C-km) is presumably below the threshold. Consequently, although the timescale of charge transfer also plays a critical role in the sprite initiation and streamer development (Hiraki & Fukunishi, 2006; Qin et al., 2013), the threshold for prompt sprite production over Matthew on 1 October is inferred to be between +250 and +350 C-km. The numerical modeling shows that positive streamers (which develop downward in sprites produced by positive CGs) require a smaller ambient electric field to initiate than negative streamers (Liu et al., 2012). Qin et al. (2013) estimated the typical critical charge moment change for the production of positive and negative sprites to be +320 and −500 C-km, respectively. We use these values for the further analysis, although it is noted that under favorable ionospheric conditions (e.g., inhomogeneities and relatively high altitude of ionosphere), the threshold for positive and negative sprite production could drop to +200 and −320 C-km, respectively (Qin et al., 2012).

Figure 4 shows the histogram of lightning strength (in terms of iCMC) for WWLLN strokes located in the eyewall and outer rainbands, respectively, during the 4-hr time interval (0430–0840UTC) of sprite observations. According to the polarity of induced ULF magnetic fields, the majority of WWLLN lightning discharges detected in the eyewall region are of negative polarity. There is no observation of any WWLLN-detected lightning with an estimated iCMC exceeding the threshold for sprite production, which may explain the absence of sprite-producible CGs in the eyewall. The iCMC produced by negative strokes appears to be generally larger than positive strokes. Our result is consistent with Thomas et al. (2010), who examined the iCMCs of WWLLN-detected lightning strokes in the inner core area (defined as the region within 100 km of the eyewall center) of three North Atlantic hurricanes. Their results show the dominance of negative strokes in the inner core, and both the peak current and iCMC of negative CGs are generally larger than for positive strokes, yet sprite-producible lightning strokes are rare in this region.

The WWLLN detected substantially more (by a factor of ~26) lightning discharges in the outer rainbands, and the predominance of negative lightning is more distinct. As shown in Figure 4b, there are several strokes with estimated iCMCs greater than the threshold for sprite production, including two negative CG strokes producing iCMC over −500 C-km. Therefore, our results indicate that in order to evaluate the capability of TCs to produce sprites, it is necessary to extend the analysis of Thomas et al. (2010) to the outer rainband regions.

4. Why No Observation of Negative Sprites?

Sprites produced by negative CGs are very rare in the land areas (Li et al., 2012), which has been largely attributed to the lack of sufficiently strong negative strokes (with large iCMCs) produced by continental thunderstorms (Cummer & Lyons, 2005). The observations of sprites on the spaceborne platform ISUAL during a 12-year period (2004–2015) suggest that a significant proportion (>80%) of negative sprites

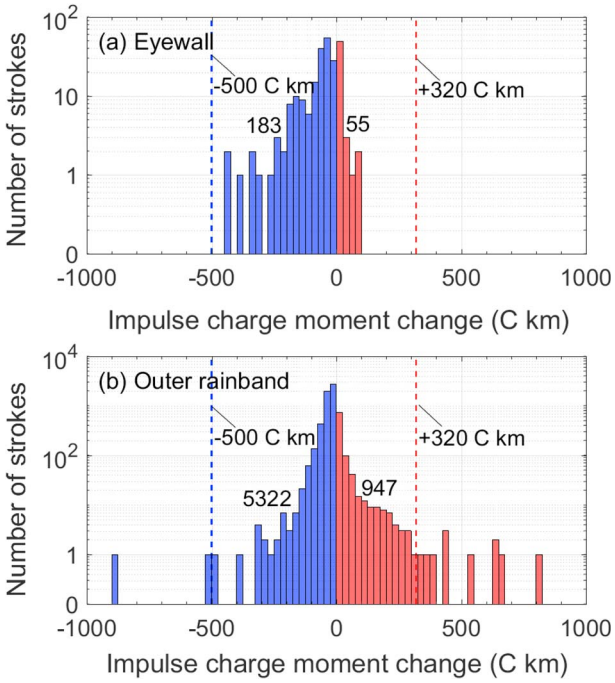

Figure 4. Histogram (in 25-C-km bins) of impulse charge moment change estimated for positive (red bins) and negative (blue bins) strokes detected by World-Wide Lightning Location Network in the (a) eyewall and (b) outer rainbands of Matthew during the main sprite observation (from 0330UTC to 0730UTC) on 1 October 2016.

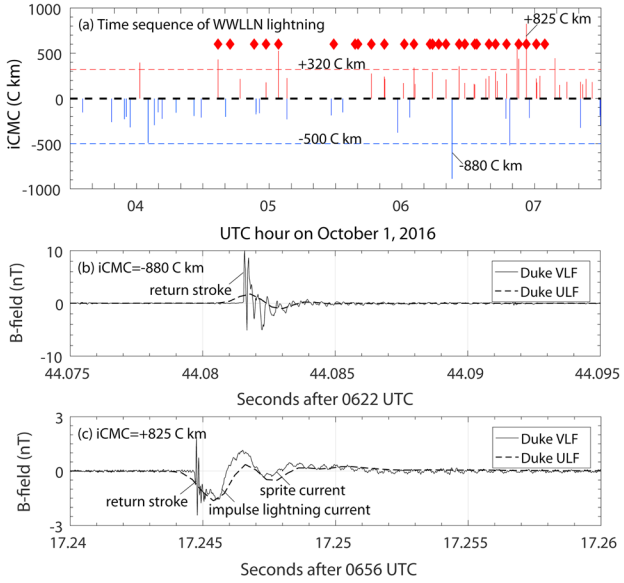

Figure 5. (a) Time sequence of World-Wide Lightning Location Network (WWLLN) lightning strokes with estimated impulse charge moment change (iCMC) $>$ ±150 C-km located in the outer rainbands during the main period of sprite observations (from 0330UTC to 0730UTC) on 1 October 2016. The red diamonds mark the observation of red sprites, and the red and blue lines indicate positive and negative WWLLN strokes, respectively. (b and c) The broadband magnetic signals measured near Duke University for the WWLLN stroke producing the largest negative iCMC and positive iCMC are plotted.

were produced in tropical oceanic/coastal thunderstorms (Lu et al., 2017). In particular, in the vast oceanic area to the north of Venezuela, only negative sprites have been observed, which is also shown by Williams et al. (2012; Figure 1). Therefore, it appears intriguing that none of the sprites observed over Matthew reported in this paper was of negative polarity.

Figure 5a shows the history for the occurrence of WWLLN lightning discharges in the outer rainbands with relatively large iCMCs (e.g., $>$ ±150 C-km). There were in total nine WWLLN discharges producing iCMC $>$ + 320 C-km, six of which were associated with reported sprite observations. During the 4-hr period shown in Figure 5a, there were only two negative strokes that produced iCMC over −500 C-km, with values of −511 and −880 C-km, respectively. Figure 5b shows the sferic signals measured at about 2,700-km range associated with the largest negative iCMC, and the broadband magnetic field for the largest positive iCMC examined in Figure 3 is shown in Figure 5c for comparison. We can see for the negative CG stroke, the VLF signal is dominated by that radiated by the return stroke, and there is no clear signature of an impulse lightning current with millisecond duration as observed for the positive CG stroke. Therefore, although the iCMCs produced by two strokes are similar, the timescale for the charge transfer of the negative stroke ($<$1 ms) was significantly shorter than that of the positive stroke (about 2 ms).

The occurrence of sprites is the consequence of conventional dielectric breakdown that persists for a sufficiently long time so that there is considerable development of streamers (Liu et al., 2009; Qin et al., 2013). Although the minimum iCMC for triggering negative sprites is estimated to be −320 C-km (Qin et al., 2012), the iCMC produced by negative sprite-producing CG strokes usually exceeds −450 C-km (Boggs et al., 2016; Li et al., 2012), which is much higher than the typical threshold (around +300 C-km) for positive sprite-producing iCMCs (e.g., Lu et al., 2017). The streamers of negative sprites are usually dim and terminate at relatively high altitude (Li et al., 2012), indicating the excitation by a lightning current with relatively short timescale ($<$0.5 ms for the cases examined by Li et al., 2012, and Liu et al., 2016). Therefore, it is possible that for the negative CGs in Figure 5a with iCMCs exceeding the threshold of sprite production, the timescale of charge transfer after the return stroke was not sufficiently long to initiate streamers.

A similar analysis is conducted for WWLLN strokes located in the inner core and outer rainbands of Matthew on October 2, when the lightning activity had significantly weakened, without finding evidence for the occurrence of negative sprites. In summary, Matthew was not considerably potential to produce negative sprites during two nights of observations. Whether or not it is typical for TCs remains to be examined. Also, Matthew may not have been typical of sprite-producing thunderstorms in the Caribbean Sea. Further ground-based observations are desired to characterize various types of sprite-producing oceanic/coastal thunderstorms.

5. Conclusions

Contributions from citizen scientists have been highly beneficial for extending the scope of scientific research on transient luminous

events. In this paper, by combining ground-based sprite observations with concurrent measurements of broadband sferics near Duke University, we examined the causative strokes of 42 sprites captured above Hurricane Matthew on the nights of 1 and 2 October as it passed to the north of Venezuela. All these sprites were produced by positive CGs located in the outer rainbands where most WWLLN lightning was detected. The sprite-producing strokes were usually located in the coldest cloud top regions with brightness temperature $\leq$194 K. The inner core containing much less lightning did not produce CG strokes with iCMCs suitable for generating sprites, consistent with previous analysis of Thomas et al. (2010).

The absence of sprites produced by negative CGs in the reported observations is contrary to the space-born observations showing that the same geographic region might be dominated by negative sprites. Therefore, further efforts are desired to characterize the typical sprite-producing meteorological systems in this area. It remains necessary to conduct ongoing ground observations to document the oceanic/coastal thunderstorms responsible for the population of negative sprites. In particular, the negative sprite-producing lightning often involves a significant progression of negative lightning leaders in the upper positive region of normally electrified thunderstorms (Boggs et al., 2016). Is this more often in oceanic/coastal thunderstorms?

Acknowledgments
This work was supported by the National Key R&D Program (2017YFC1501501) and National Natural Science Foundation of China (41574179 and 41622501). The Watec 902H Ultimate camera system used to capture the B&W image of sprite was purchased by John Mathews of Penn State University under NSF grant 12-02019. The data examined in the paper are available at https://doi.org/10.5281/zenodo.1434501.

References

Abarca, S. F., Corbosiero, K. L., & Galarneau, T. J. Jr. (2010). An evaluation of the Worldwide Lightning Location Network (WWLLN) using the National Lightning Detection Network (NLDN) as ground truth. *Journal of Geophysical Research*, *115*, D18206. https://doi.org/10.1029/2009JD013411

Boccippio, D. J., Williams, E. R., Heckman, S. J., Lyons, W. A., Baker, I. T., & Boldi, R. (1995). Sprites, ELF transients and positive ground strokes. *Science*, *269*(5227), 1088–1091. https://doi.org/10.1126/science.269.5227.1088

Boggs, L. D., Liu, N., Splitt, M., Lazarus, S., Glenn, C., Rassoul, H., & Cummer, S. A. (2016). An analysis of five negative sprite-parent discharges and their associated thunderstorm charge structures. *Journal of Geophysical Research: Atmospheres*, *121*, 759–784. https://doi.org/10.1002/2015JD024188

Chen, A. B., Kuo, C. L., Lee, Y. J., Su, H. T., Hsu, R. R., Chern, J. L., et al. (2008). Global distributions and occurrence rates of transient luminous events. *Journal of Geophysical Research*, *113*, A08306. https://doi.org/10.1029/2008JA013101

Christian, H. J., Blakeslee, R. J., Goodman, S. J., Mach, D. A., Stewart, M. F., Buechler, D. E., et al. (2003). Global frequency and distribution of lightning as observed from space by the Optical Transient Detector. *Journal of Geophysical Research*, *108*(D1), 4005. https://doi.org/10.1029/2002JD002347

Cummer, S. A., Inan, U. S., Bell, T. F., & Barrington-Leigh, C. P. (1998). ELF radiation produced by electrical currents in sprites. *Geophysical Research Letters*, *25*(8), 1281–1284. https://doi.org/10.1029/98GL50937

Cummer, S. A., & Lyons, W. A. (2005). Implications of lightning charge moment changes for sprite initiation. *Journal of Geophysical Research*, *110*, A04304. https://doi.org/10.1029/2004JA010812

Davis, C. J., & Johnson, C. (2005). Lightning-induced intensification of the ionospheric sporadic E layer. *Nature*, *435*(7043), 799–801. https://doi.org/10.1038/nature03638

Didlake, A. C. Jr., & Kumjian, M. R. (2017). Examining polarimetric radar observations of bulk microphysical structures and their relation to vortex kinematics in Hurricane Arthur (2014). *Monthly Weather Review*, *145*(11), 4521–4541. https://doi.org/10.1175/MWR-D-17-0035.1

Füllekrug, M., Price, C., Yair, Y., & Williams, E. R. (2002). Intense oceanic lightning. *Annales de Geophysique*, *20*(1), 133–137. https://doi.org/10.5194/angeo-20-133-2002

Harr, P. A., & Elsberry, R. L. (1996). Structure of a mesoscale convective system embedded in Typhoon Robyn during TCM-93. *Monthly Weather Review*, *124*(4), 634–652. https://doi.org/10.1175/1520-0493(1996)124<0634:SOAMCS>2.0.CO;2

Hiraki, Y., & Fukunishi, H. (2006). Theoretical criterion of charge moment change by lightning for initiation of sprites. *Journal of Geophysical Research*, *111*, A11305. https://doi.org/10.1029/2006JA011729

Houze, R. A. Jr. (2010). Clouds in tropical cyclones. *Monthly Weather Review*, *138*(2), 293–344. https://doi.org/10.1175/2009MWR2989.1

Huang, A., Lu, G., Zhang, H., Liu, F., Fan, Y., Zhu, B., et al. (2018). Locating parent lightning strokes of sprites observed over a mesoscale convective system in Shandong Province, China. *Advances in Atmospheric Sciences*, *35*(11), 1396–1414. https://doi.org/10.1007/s00376-018-7306-4

Huang, S.-M., Hsu, R.-R., Lee, L.-J., Su, H.-T., Kuo, C.-L.,Wu, C.-C., & Chen, A. B. (2012). Optical and radio signatures of negative gigantic jets: Cases from Typhoon Lionrock (2010). *Journal of Geophysical Research*, *117*, A08307. https://doi.org/10.1029/2012JA017600

Li, J., Cummer, S., Lu, G., & Zigoneanu, L. (2012). Charge moment change and lightning-driven electric fields associated with negative sprites and halos. *Journal of Geophysical Research*, *117*, A09310. https://doi.org/10.1029/2012JA017731

Liu, N., Kosar, B., Sadighi, S., Dwyer, J. R., & Rassoul, H. K. (2012). Formation of streamer discharges from an isolated ionization column at sub-breakdown conditions. *Physical Review Letters*, *109*(2), 025002. https://doi.org/10.1103/PhysRevLett.109.025002

Liu, N. Y., Boggs, L. D., & Cummer, S. A. (2016). Observation-constrained modeling of the ionospheric impact of negative sprites. *Geophysical Research Letters*, *43*, 2365–2373. https://doi.org/10.1002/2016GL068256

Liu, N. Y., Dwyer, J. R., Stenbaek-Nielsen, H. C., & McHarg, M. G. (2015). Sprite streamer initiation from natural mesospheric structures. *Nature Communications*, *6*(1), 7540. https://doi.org/10.1038/ncomms8540

Liu, N. Y., Pasko, V. P., Adams, K., Stenbaek-Nielsen, H. C., & McHarg, M. G. (2009). Comparison of acceleration, expansion, and brightness of sprite streamers obtained from modeling and high-speed video observations. *Journal of Geophysical Research*, *114*, A00E03. https://doi.org/10.1029/2008JA013720

Liu, N. Y., Spiva, N., Dwyer, J. R., Rassoul, H. K., Free, D., & Cummer, S. A. (2015). Upward electrical discharges observed above Tropical Depression Dorian. *Nature Communications*, *6*(1), 5995. https://doi.org/10.1038/ncomms6995

Lu, G., Cummer, S. A., Blakeslee, R. J., Weiss, S., & Beasley, W. H. (2012). Lightning morphology and impulse charge moment change of high peak current negative strokes. *Journal of Geophysical Research*, *117*, D04212. https://doi.org/10.1029/2011JD016890

Lu, G., Cummer, S. A., Chen, A. B., Lyu, F., Huang, S., Hsu, R. R., & Su, H. T. (2017). Analysis of lightning strokes associated with sprites observed from space in North America. *Terrestrial, Atmospheric and Oceanic Sciences*, *28*(4), 583–595. https://doi.org/10.3319/TAO.2017.03.31.01

Lu, G., Cummer, S. A., Li, J., Zigoneanu, L., Lyons, W. A., Stanley, M. A., et al. (2013). Coordinated observations of sprites and in-cloud lightning flash structure. *Journal of Geophysical Research: Atmospheres*, *118*, 6607–6632. https://doi.org/10.1002/jgrd.50459

Lyons, W. (1996). Sprite observations above the U.S. High Plains in relation to their parent thunderstorm systems. *Journal of Geophysical Research*, *101*(D23), 29,641–29,652. https://doi.org/10.1029/96JD01866

Lyons, W. A., & Keen, C. S. (1994). Observations of lightning in convective super-cells within tropical storms and hurricanes. *Monthly Weather Review*, *122*(8), 1897–1916. https://doi.org/10.1175/1520-0493(1994)122<1897:OOLICS>2.0.CO;2

Marshall, R. A., Yue, J., & Lyons, W. A. (2015). Numerical simulation of an elve modulated by a gravity wave. *Geophysical Research Letters*, *42*, 6120–6127. https://doi.org/10.1002/2015GL064913

Miller, S., Straka, W., Yue, J., Seaman, C., Xu, S., Elvidge, C., et al. (2018). The dark side of Hurricane Matthew: Unique perspectives from the VIIRS day/night band. *Bulletin of the American Meteorological Society*. https://doi.org/10.1175/BAMS-D-17-0097.1

Molinari, J., Moore, P., & Idone, V. (1999). Convective structure of hurricanes as revealed by lightning locations. *Monthly Weather Review*, *127*(4), 520–534. https://doi.org/10.1175/1520-0493(1999)127<0520:CSOHAR>2.0.CO;2

Neubert, T., Allin, T. H., Blanc, E., Farges, T., Haldoupis, C., Mika, A., et al. (2005). Coordinated observations of transient luminous events during the EuroSprite2003 campaign, *Journal of Atmospheric and Solar-Terrestrial Physics*, *67*, 807–820. https://doi.org/10.1016/j.jastp.2005.02.004

Pasko, V. P., Inan, U. S., Bell, T. F., & Reising, S. C. (1998). Mechanism of ELF radiation from sprites. *Geophysical Research Letters*, *25*(18), 3493–3496. https://doi.org/10.1029/98GL02631

Pasko, V. P., Inan, U. S., Bell, T. F., & Taranenko, Y. N. (1997). Sprites produced by quasi-electrostatic heating and ionization in the lower ionosphere. *Journal of Geophysical Research*, *102*(A3), 4529–4561. https://doi.org/10.1029/96JA03528

Qin, J., Celestin, S., & Pasko, V. P. (2012). Minimum charge moment change in positive and negative cloud to ground lightning discharges producing sprites. *Geophysical Research Letters*, *39*, L22801. https://doi.org/10.1029/2012GL053951

Qin, J., Celestin, S., & Pasko, V. P. (2013). Dependence of positive and negative sprite morphology on lightning characteristics and upper atmospheric ambient conditions. *Journal of Geophysical Research: Space Physics*, *118*, 2623–2638. https://doi.org/10.1029/2012JA017908

Said, R. K., Cohen, M. B., & Inan, U. S. (2013). Highly intense lightning over the oceans: Estimated peak currents from global GLD360 observations. *Journal of Geophysical Research: Atmospheres*, *118*, 6905–6915. https://doi.org/10.1002/jgrd.50508

Sato, M., & Fukunishi, H. (2003). Global sprite occurrence locations and rates derived from triangulation of transient Schumann resonance events. *Geophysical Research Letters*, *30*(16), 1859. https://doi.org/10.1029/2003GL017291

Sentman, D. D., Wescott, E. M., Osborne, D. L., Hampton, D. L., & Heavner, M. J. (1995). Preliminary results from the Sprites94 Aircraft Campaign: 1. Red sprites. *Geophysical Research Letters*, *22*(10), 1205–1208. https://doi.org/10.1029/95GL00583

Shao, X.-M., Lay, E. H., & Jacobson, A. R. (2013). Reduction of electron density in the night-time lower ionosphere in response to a thunderstorm. *Nature Geoscience*, *6*(1), 29–33. https://doi.org/10.1038/ngeo1668

Soula, S., van der Velde, O., Montanyà, J., Neubert, T., Chanrion, O., & Ganot, M. (2009). Analysis of thunderstorm and lightning activity associated with sprites observed during the EuroSprite campaigns: Two case studies. *Atmospheric Research*, *91*(2–4), 514–528. https://doi.org/10.1016/j.atmosres.2008.06.017

Stewart, S. R. (2017). Hurricane Matthew (AL142016) 28 September–9 October 2016. National Hurricane Center Tropical Cyclone Report, 88 pp.

Su, H.-T., Hsu, R. R., Chen, A. B., Lee, Y. J., & Lee, L. C. (2002). Observation of sprites over the Asian continent and over oceans around Taiwan. *Geophysical Research Letters*, *29*(4), 1044. https://doi.org/10.1029/2001GL013737

Taranenko, Y. N., Inan, U. S., & Bell, T. F. (1993). The interaction with the lower ionosphere of electromagnetic pulses from lightning: Excitation of optical emissions. *Geophysical Research Letters*, *20*(23), 2675–2678. https://doi.org/10.1029/93GL02838

Thomas, J. N., Solorzano, N. N., Cummer, S. A., & Holzworth, R. H. (2010). Polarity and energetics of inner core lightning in three intense North Atlantic hurricanes. *Journal of Geophysical Research*, *115*, A00E15. https://doi.org/10.1029/2009JA014777

Williams, E., Kuo, C. L., Bór, J., Sátori, G., Newsome, R., Adachi, T., et al. (2012). Resolution of the sprite polarity paradox: The role of halos. *Radio Science*, *47*, RS2002. https://doi.org/10.1029/2011RS004794

Wu, W., Rutledge, S. A., & Zhang, W. (2017). Relationships between total lightning, deep convection, and tropical cyclone intensity change. *Journal of Geophysical Research: Atmospheres*, *122*, 7047–7063. https://doi.org/10.1002/2017JD027072

Xu, L., Zhang, Y., Wang, F., & Zheng, D. (2014). Simulation of the electrification of a tropical cyclone using the WRF-ARW model: An idealized case. *Journal of Meteorological Research*, *28*(3), 453–468. https://doi.org/10.1007/s13351-014-3079-6

Yang, J., Qie, X., & Feng, G. (2013). Characteristics of one sprite-producing summer thunderstorm. *Atmospheric Research*, *127*, 90–115. https://doi.org/10.1016/j.atmosres.2011.08.001

Yu, B., Xue, X., Lu, G., Kuo, C. L., Dou, X., Gao, Q., et al. (2017). The enhancement of neutral metal Na layer above thunderstorms. *Geophysical Research Letters*, *44*,9555–9563.. https://doi.org/10.1002/2017GL074977

Yue, J., & Lyons, W. A. (2015). Structured elves: Modulation by convectively generated gravity waves. *Geophysical Research Letters*, *42*, 1004–1011. https://doi.org/10.1002/2014GL062612

Zhang, W., Zhang, Y., Zheng, D., Wang, F., & Xu, L. (2015). Relationship between lightning activity and tropical cyclone intensity over the northwest Pacific. *Journal of Geophysical Research: Atmospheres*, *120*, 4072–4089. https://doi.org/10.1002/2014JD022334